TITLE
ASP Conference Series, Vol. **VOLUME**, **PUBLICATION YEAR**
EDITORS

Radio Pulsar Polarimetry

I. H. Stairs

NRAO, P.O. Box 2, Green Bank, WV 24944 U.S.A.

Abstract. Radio pulsars emit highly polarized radiation, which can be used as a unique tool in many astrophysical experiments. This article describes instrumentation for polarization observations of radio pulsars, discusses the polarimetric properties of pulsars in general and summarizes some astrophysical applications of pulsar polarimetry.

Introduction

Radio pulsars were discovered in 1967 (Hewish et al. 1968) and were soon identified as rapidly rotating, highly magnetized neutron stars. These objects present an extreme stellar environment, with nuclear densities, spin periods between 1.5 ms and 8.5 s, and surface magnetic fields ranging from 10^8 G to more than 10^{13} G. A pulsar produces broadband beamed radio emission; when the beam crosses the line of sight to the earth, "pulses" are observed. Over the years, it has been recognized that, subject to a spin-down model discussed below, pulsars form extremely stable clocks. As such, they have been used for a wide range of astrophysical experiments, from setting limits on the internal structure of neutron stars, to studying the dynamics of binary systems, to performing stringent tests of the predictions of general relativity.

Much information can also be gained from studying the shapes of pulse profiles and the polarization properties of pulsars. In fact, pulsars tend to be highly polarized, showing both circular and linear polarization, and with polarized fractions of up to 100%. Pulsars are generally weak, steep-spectrum objects, with typical peak flux densities of around 10 mJy at a few hundred MHz, necessitating the use of radio telescopes with large collecting areas.

This paper will summarize the observing techniques used in pulsar polarization studies, then discuss the polarimetric properties of pulsars and some of the astrophysical experiments that can be performed with such observations.

Instrumentation

The primary concern of any pulsar instrument is overcoming the effects of interstellar dispersion. The ionized interstellar medium (ISM) acts as a frequency-dependent retarding filter on the pulsed signal, with the result that signals at low frequencies arrive later than their higher-frequency counterparts. The delay Δt in seconds expected between signals at two frequencies ν_1 and ν_2 in MHz may be written as:

$$\Delta t = \frac{1}{2.41 \times 10^{-4}} \mathrm{DM} \left(\frac{1}{\nu_1^2} - \frac{1}{\nu_2^2} \right), \tag{1}$$

where the dispersion measure, given by $\mathrm{DM} = \int_0^d N_e dz$, is the integrated electron density along the line of sight to the pulsar, usually measured in $\mathrm{cm}^{-3}\mathrm{pc}$. Over typical observing bandwidths, the total delay can amount to hundreds or even thousands of times the intrinsic pulse width.

The traditional approach to removing dispersion has been to employ a filterbank system, or other spectrometer, in which the observing bandpass is split into multiple small channels, and the signal is detected in each channel before being shifted by the predicted dispersive delay to realign the pulse. While this analog method operates in real time, a significant disadvantage lies in the unavoidable residual dispersive smearing within each frequency channel.

Hardware polarimeters are used with filterbank instruments. These fall into two categories: adding and multiplying polarimeters. Adding polarimeters are typically passive devices which sum the input voltages, in phase and rotated by $90°$, producing outputs such as R, L, $R+L$ and $R+iL$ for input right- and left-circular polarizations R and L. As the signals are not detected in the process, an adding polarimeter may be used before the signals are passed to the filterbank. Stokes parameters may then be calculated once the outputs have been filtered and detected. Multiplying polarimeters perform signal detection and multiplication in hardware, typically yielding $|R|^2$, $|L|^2$, $\mathrm{Re}(L^*R)$ and $\mathrm{Im}(L^*R)$; a separate polarimeter must therefore be used for each filterbank channel. See von Hoensbroech & Xilouris (1997) for a thorough description of hardware polarimeter calibration at the Effelsberg 100-m telescope.

Correlator-style instruments produce self- and cross-product correlation functions after sampling the incoming voltages; the resultant data products are therefore similar to those produced by a filterbank plus multiplying polarimeter. See Navarro (1994) for an example.

A superior method of removing the ISM smearing is a procedure known as coherent dedispersion, pioneered by Hankins & Rickett (1975). The effects of the ISM plasma on the propagating pulsar signal can be simply described as a frequency-domain "chirp" filter, dependent primarily on the pulsar's dispersion measure. The coherent dedispersion technique involves mixing the incoming telescope voltages to baseband, Nyquist-sampling the data streams, and then convolving the time series with the inverse of the ISM chirp function. The data streams are then detected, and calibration is straightforward. If two polarizations are observed, suitable cross-products will yield the Stokes parameters, giving full polarimetric information at the same time. This technique completely eliminates the effects of dispersion. A comparison between filterbank and coherent dedispersion observations can be seen in Fig. 1.

Coherent dedispersion can be implemented in hardware or software. Hardware systems use special-purpose chips to convolve the data stream with the inverse chirp function, and then typically fold the dedispersed data, greatly reducing the overall data rate (e.g., Stinebring et al. 1992, Backer et al. 1997); An alternative is to record the baseband time series and carry out the deconvolution in software (e.g., Jenet et al. 1997, Stairs et al. 2000). This approach more easily

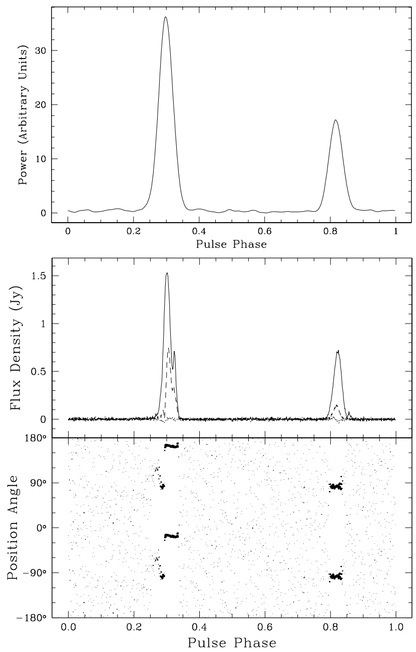

Figure 1. Pulse profile of the fastest rotating pulsar, PSR B1937+21, observed with the 76-m Lovell telescope at Jodrell Bank Observatory, U.K. The top panel shows the total-intensity profile derived from a filterbank observation; the true profile shape is convolved with the response of the channel filters. The lower panels shows the full-Stokes observation with a coherent dedispersion instrument (Stairs, Thorsett, & Camilo 1999). Here, and in the following figures, total intensity is indicated by a solid line, linear intensity by a dashed line, and circular power by a dotted line. The position angle is plotted twice for clarity.

permits software interference excision and reprocessing of the data to account for DM changes or to examine single pulses. With increasing computer speeds, this software approach is becoming more and more routinely usable.

Instrumental Effects and Corrections

For telescopes that are not equatorially mounted, the Stokes Q and U parameters are affected by the parallactic rotation of the feed during tracking. For a given hour angle, telescope latitude and source declination, the parallactic angle χ is easily calculated (Rankin, Campbell, & Spangler 1975), and the correct parameters can be recovered by rotating the (Q,U) pair by the angle 2χ. The corrected Q, U values may then be used to derive the linearly polarized power L and source position angle ψ.

A further complication arises from the fact that, in general, receiver antennas are not perfectly orthogonal, nor, in the case of "circular" antennas, perfectly responsive to circularly polarized radiation. This results in a mixing of the Stokes parameters, so that the observed Stokes vector is the product of the true Stokes vector and the Mueller matrix, and can result in significant distortion of the pulse polarimetry. It is possible to correct for this cross-coupling; in fact pulsars can be used to calculate the Mueller matrix for a receiver (Xilouris 1991). A first-order correction can be found following the method of Stinebring (1982), in which it is assumed that the circular antennas are elliptical but orthogonal. The most significant effect is then mixing between L and V, sinusoidally dependent on the incident position angle of the radiation. For strongly linearly polarized pulsars, it is assumed that $L_{\rm observed} \simeq L$. Then the mixing parameters can be determined by fitting a sinusoid to $V_{\rm observed}/L$. Once the cross-coupling parameters have been determined using a strong pulsar, they can be used to correct L and V for all pulsars observed with the same system.

Stokes parameter mixing can also be induced by differences in path length from the antenna to the detector. This will mix Q and U for circular antennas, resulting in a measurable position angle offset, and U and V for linear antennas. In the latter case, the problem can be corrected by summing Stokes parameters taken with the antennas offset by a 90° rotation.

Polarimetric Properties of Pulsars

Although the radio pulsar emission mechanism is poorly understood, a fairly successful model is that of a rotating magnetic dipole. From pulse timing observations, the spin period P and period derivative $\dot{P}$ can be measured; under the magnetic dipole assumption, these lead to estimates of the pulsar's characteristic age ($\tau = P/(2\dot{P})$ s) and surface magnetic field ($B = 3.2 \times 10^{19} (P\dot{P})^{1/2}$ G). For a misaligned dipole, there will be a set of field lines above the polar caps which cannot close without rotating at a speed above that of light. The basic picture of radio emission then involves coherent curvature radiation from charged particles streaming along these open field lines (Goldreich & Julian 1969).

It was soon realized (Radhakrishnan & Cooke 1969) that the position angle of linearly polarized emission from such a rotating dipole should follow a well-defined "S"-shaped curve, in what is known as the "rotating vector model" (RVM). The exact shape of the predicted curve depends on the inclination α of the magnetic dipole axis relative to the spin axis and on the impact parameter β between the dipole axis and our line of sight. The position angle ψ can be written as a function of pulse phase ϕ:

$$\tan(\psi(\phi) - \psi_0) = \frac{\sin\alpha \sin(\phi - \phi_0)}{\cos\alpha \sin(\zeta) - \sin\alpha \cos(\zeta) \cos(\phi - \phi_0)}, \quad (2)$$

where $\zeta = \alpha + \beta$, ψ_0 is a constant offset and ϕ_0 is the phase of steepest position-angle swing.

A large number of pulsars fit the RVM quite well, for example, that shown in the left panel of Fig. 2. In these cases, it is usually possible to obtain a good fit for β; in practice, fitting for α requires additional position angle information at pulse phases outside the main pulse, for instance in an interpulse.

The large set of polarimetric pulse profiles has led, over the years, to phenomenological models of the pulse emission region for young pulsars (e.g., Rankin 1983, 1990, 1993, Lyne & Manchester 1988). Different strengths of polarization

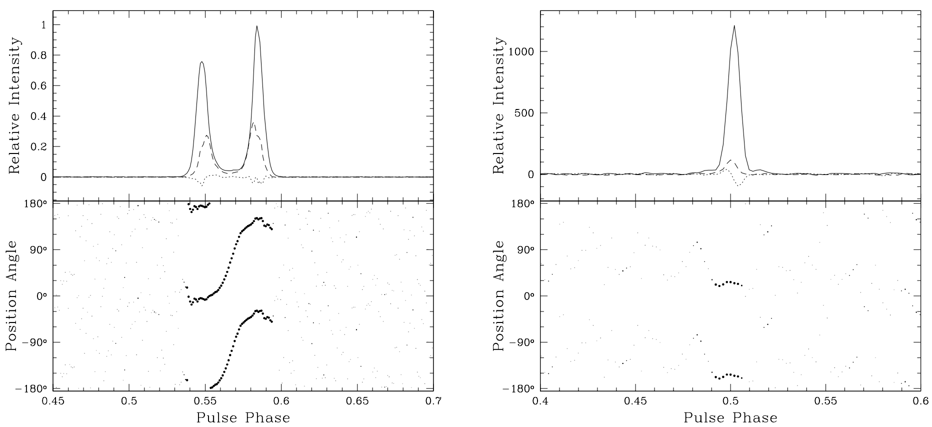

Figure 2. Examples of conal and core emission. Left panel: conal emission from PSR B0525+21 observed at 1410 MHz at Effelsberg (data from von Hoensbroech & Xilouris 1997). Right panel: core emission from PSR B2002+31, observed at 610 MHz at Jodrell Bank (data from Gould & Lyne 1998).

and different characteristics of position angle swing are associated with different types of emission. The two basic varieties of integrated pulse profiles are labeled "conal" and "core" emission.

An example of conal emission is shown in the left panel of Fig. 2. Radiation is produced in a hollow ring centred on the dipole axis, typically yielding a double-peaked profile as seen in the figure. Conal emission is associated with strong linear polarization and a position angle swing that follows the RVM. There is usually little circular power, however, and the spectral index is comparatively shallow. Double cones may sometimes be seen. The profile components tend to shift closer together at higher observing frequencies, and may merge.

The right panel of Fig. 2 displays an example of core emission, thought to originate in a single patch centred on the dipole axis. This type of emission contains only weak linear power, and the position angle swing may be quite steep, or else irregular. The circular power is usually strong, and may change sign at the midpoint of the profile. Core emission usually has a steep spectral index, especially for short-period pulsars.

Many pulse profiles contain a mixture of cone and core components, leading to significant evolution with observing frequency. The overall fraction of polarized emission also tends to decrease with observing frequency. Some pulsars exhibit mode changing – discrete switching between two or more different profiles on timescales of minutes or hours (e.g., Backer 1970a) – or nulling, in which a pulsar will simply cease to emit radio pulses for up to a few hundred spin periods (e.g., Backer 1970b).

With RVM impact parameters (and occasionally magnetic inclination angles) measured for a large set of pulsars, attempts have been made to reconstruct the average 2-dimensional pulsar beam shape (e.g., Han & Manchester 2001). The distribution of magnetic inclination angles has also been investigated, with some debate over whether the magnetic and spin axes tend to align as pulsars age (e.g., Gil & Han 1996, Tauris & Manchester 1998).

While pulse profiles integrated over a few minutes or more are generally stable and lend themselves to the type of classification schemes discussed above, individual pulses of young pulsars are highly variable, in strength and shape, and intensity and type of polarization. Individual pulses are often composed of subpulses, which may appear at random or preferred longitudes, or else drift across the pulse (Drake & Craft 1968). On even shorter timescales a pulsar may display the phenomenon called microstructure (Craft, Comella, & Drake 1968), consisting of short, intense spikes of emission. Both subpulses and microstructure tend to be highly polarized, but when hundreds or pulses are summed to produce the average profile, the overall polarization may be much less than 100%.

Some pulsars show 90° jumps in the position angle swing, typically accompanied by a null in the linear power. Single pulse observations are the key to understanding this phenomenon. These data show that separate pulses may have position angles that differ by 90°, forming orthogonal emission modes. The average-profile position angle at any given pulse longitude is then determined by which mode dominates at that longitude. The modes are possibly disjoint (e.g., Cordes, Rankin, & Backer 1978) but appear more likely to be superimposed (McKinnon & Stinebring 1998, 2000).

The phenomenological cone/core emission models apply fairly well to young pulsars, the direct products of supernova explosions. However, there is a second class of pulsars, those which have undergone an episode of mass and angular momentum accretion from an evolving main-sequence companion. These "recycled" pulsars have spin periods as short as 1.5 ms, and magnetic fields typically only 10^8 G. See Bhattacharya & van den Heuvel (1991) for a review of binary and millisecond pulsar evolution.

Some examples of polarimetric observations of millisecond pulsars are given in Fig. 3. These and previous observations (e.g., Xilouris et al. 1998, Stairs, Thorsett, & Camilo 1999) illustrate that millisecond pulsars, though also highly polarized, do not easily match the phenomenological models. Position angle swings are often flat, or else bear little resemblance to any RVM prediction. There is often very little frequency development of the profiles, and some pulse components defy classification as cones or cores. There is increasing evidence that some millisecond pulsars show short-term changes in total intensity and/or polarization (see, e.g., Kramer et al. 1999a, Sallmen 1998).

Some Astrophysical Applications

In addition to their use in developing phenomenological emission models, polarimetric observations of pulsars can be used to test directly various ideas about the radio emission mechanism and magnetospheric propagation effects. Using a relativistic correction to the RVM which takes into account the rotation of the magnetospheric plasma, the delay between the midpoint of the profile and the point of steepest swing of the position angle can be used to estimate the height above the neutron star surface at which the radiation was emitted (Blaskiewicz, Cordes, & Wasserman 1991). Such estimates agree reasonably well with other estimates derived assuming that the narrowing of conal components with fre-

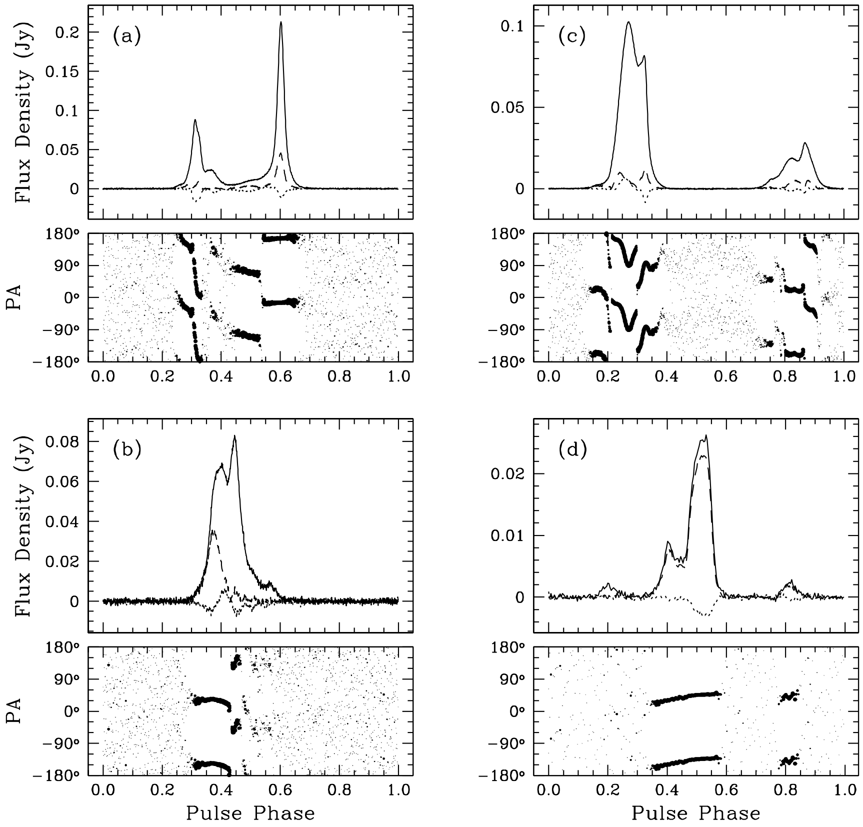

Figure 3. Arecibo polarimetric pulse profiles of millisecond pulsars: (a) PSR J0621+1002 at 430 MHz, (b) PSR B1257+12 at 430 MHz, (c) PSR B1855+09 at 1400 MHz, (d) PSR J2019+2425 at 430 MHz. (a)–(c) Stairs, unpublished, (d) Nice, Splaver, & Stairs 2001.

quency indicates a lower emission height for higher-frequency radiation (e.g., Cordes 1978). A different explanation proposes that both profile narrowing and depolarization at higher frequencies can be attributed to separate propagation of orthogonal polarization modes within the magnetospheric plasma (e.g., McKinnon 1997). However, the depolarization without significant profile evolution observed in millisecond pulsars may cast doubt on this explanation (Kramer et al. 1999b). Finally, the narrow-band profile and polarization changes observed in the millisecond pulsar J1022+1001 (Kramer et al. 1999a) may be interpretable in terms of a magnetospheric scintillation effect (Lyutikov & Parikh 2000).

Pulsar polarization measurements can also be used to deduce information about their local or galactic environments. The chief tool used here is the rotation measure, $\mathrm{RM} = \int_0^d N_e B_{\|} dz$, which measures the line-of-sight component of the magnetic field between the Earth and the pulsar, multiplied by the electron density. The RM can be determined from an observed offset in position angle across the observing bandpass: $\Delta\psi = \mathrm{RM}\,\lambda^2$, where λ is the observing wavelength. Measurement of RMs of pulsars in different galactic locations has helped investigations of the structure of the Galactic magnetic field (e.g., Han, Manchester, & Qiao 1999). The orbital variation of the pulsar's RM has led to a measurement of the magnetic field strength of the Be-star companion to PSR B1259−63 (Johnston et al. 1996) and may eventually yield similar information about the unidentified companion to the recently discovered PSR J1740−3052 (Stairs et al. 2001). In eclipsing pulsar–white dwarf binaries, changes in linear polarization strength with orbital phase, if found, can test the predictions of eclipse mechanism models (e.g., Khechinashvili, Melikidze, & Gil 2000).

A further application of polarimetric profiles, dependent on RVM results, is in obtaining constraints on the orbital geometry of binary pulsars. In particular, the relativistic double-neutron-star system PSRs B1913+16 is very well studied and has allowed determination of the sine of orbital inclination angle through measurement of relativistic timing parameters (Taylor & Weisberg 1989). The pulsar's spin axis is also undergoing geodetic precession, resulting in long-term secular evolution of the pulse profile shape (e.g. Weisberg, Romani, & Taylor 1989). Kramer (1998) has used the long-term narrowing of the profile to determine the magnetic inclination and the spin-orbit misalignment angle. Knowledge of the sign of the RVM impact parameter (Cordes, Wasserman & Blaskiewicz 1990) breaks a degeneracy between the possible solutions and allows the formulation of a complete picture of the orbital and spin geometry of the system.

With more data now being acquired by the high-precision coherent dedispersion instruments, there is hope for similar geometric constraints being placed on other systems in the future . Another exciting prospect, made possible by the routine acquisition of full-Stokes profiles, is the use of polarization information to increase the precision of pulsar timing measurements.

Acknowledgments

The data for the profiles in Fig. 2 were obtained from the European Pulsar Network data archive. IHS is supported by an NRAO Jansky fellowship. She thanks the organizers of the workshop for the invitation to speak, and Michael Kramer and Dick Manchester for reading the manuscript.

References

Backer, D. C. 1970a, Nature, 228, 1297

Backer, D. C. 1970b, Nature, 228, 42

Backer, D. C. et al. 1997, PASP, 109, 61

Bhattacharya, D. & van den Heuvel, E. P. J. 1991, Phys. Rep., 203, 1

Blaskiewicz, M., Cordes, J. M., & Wasserman, I. 1991, ApJ, 370, 643

Cordes, J. M. 1978, ApJ, 222, 1006

Cordes, J. M., Rankin, J. M., & Backer, D. C. 1978, ApJ, 223, 961

Cordes, J. M., Wasserman, I., & Blaskiewicz, M. 1990, ApJ, 349, 546

Craft, H. D., Comella, J. M., & Drake, F. 1968, Nature, 218, 1122

Drake, F. D. & Craft, H. D. 1968, Nature, 220, 231
Gil, J. A. & Han, J. L. 1996, ApJ, 458, 265
Goldreich, P. & Julian, W. H. 1969, ApJ, 157, 869
Gould, D. M. & Lyne, A. G. 1998, MNRAS, 301, 235
Han, J. L. & Manchester, R. N. 2001, MNRAS, 320, L35
Han, J. L., Manchester, R. N., & Qiao, G. J. 1999, MNRAS, 306, 371
Hankins, T. H. & Rickett, B. J. 1975, in Methods in Computational Physics Volume 14 — Radio Astronomy (New York: Academic Press), 55
Hewish, A. et al. 1968, Nature, 217, 709
Jenet, F. A. et al. 1997, PASP, 109, 707
Johnston, S. et al. 1996, MNRAS, 279, 1026
Khechinashvili, D. G., Melikidze, G. M., & Gil, J. A. 2000, ApJ, 541, 335
Kramer, M. 1998, ApJ, 509, 856
Kramer, M. et al. 1999a, ApJ, 520, 324
Kramer, M. et al. 1999b, ApJ, 526, 957
Kramer, M. et al. 1997, A&A, 322, 846
Lyne, A. G. & Manchester, R. N. 1988, MNRAS, 234, 477
Lyutikov, M. & Parikh, A. 2000, ApJ, 541, 1016
McKinnon, M. 1997, ApJ, 475, 763
McKinnon, M. M. & Stinebring, D. R. 1998, ApJ, 502, 883
McKinnon, M. M. & Stinebring, D. R. 2000, ApJ, 529, 435
Navarro, J. 1994. PhD thesis, California Institute of Technology
Nice, D. J., Splaver, E. M., & Stairs, I. H. 2001, ApJ, In press, astro-ph/0010489
Radhakrishnan, V. & Cooke, D. J. 1969, Astrophys. Lett., 3, 225
Rankin, J. M. 1983, ApJ, 274, 333
Rankin, J. M. 1990, ApJ, 352, 247
Rankin, J. M. 1993, ApJ, 405, 285
Rankin, J. M., Campbell, D. B., & Spangler, S. R. 1975, NAIC Report 46
Sallmen, S. 1998. PhD thesis, University of California at Berkeley
Stairs, I. H. et al. 2001, MNRAS. In press, astro-ph/0012414
Stairs, I. H. et al. 2000, MNRAS, 314, 459
Stairs, I. H., Thorsett, S. E., & Camilo, F. 1999, ApJS, 123, 627
Stinebring, D. R. 1982. PhD thesis, Cornell University
Stinebring, D. R. et al. 1992, Rev. Sci. Instrum., 63, 3551
Tauris, T. M. & Manchester, R. N. 1998, MNRAS, 298, 625
Taylor, J. H. & Weisberg, J. M. 1989, ApJ, 345, 434
von Hoensbroech, A. & Xilouris, K. M. 1997, A&AS, 126, 121
Weisberg, J. M., Romani, R. W., & Taylor, J. H. 1989, ApJ, 347, 1030
Xilouris, K. M. 1991, A&A, 248, 323
Xilouris, K. M. et al. 1998, ApJ, 501, 286

Discussion

Wade: For Magnetic Ap stars, one important realization made during the last 5–10 years is that their fields are definitely not dipolar. What are the prospects for using radio polarimetry (or other observations) to develop more realistic models of pulsar magnetic fields?
Stairs: While the dipole model may not be perfect, it is certainly a plausible approximation in many cases. However, there has been much speculation that millisecond pulsars in particular, with compact magnetospheres, beams that are often narrower and less prone to frequency development than predicted by the core/cone model, and complex position angle swings, may have significant non-dipolar contributions. Nevertheless, the good alignment of pulse profiles with frequency, based on a timing model and dispersion measure measurement, for both young and millisecond pulsars, implies a collimation of the emission regions at different frequencies and hence, it can be argued, no significant displacement from alignment with a dipole axis (e.g., Kramer et al. 1997, 1999b).
Wade: Are there any nice orthogonal diagnostics of magnetic fields in pulsars (like the Zeeman effect for non-degenerate stars) or is it all just a mish-mash?
Stairs: There is admittedly nothing as well-defined as the Zeeman effect. We determine the strength and geometry of the magnetic field as best we can using the tools we have: the dipolar spin-down timing model and fits to the position angle swing across the pulse profile.
Mathys: Could the methods that you described in your talk be used to study the magnetic fields of the most strongly magnetic white dwarfs?
White: White dwarfs don't emit in the radio.
Stairs: Also, the information needed (spin-down timing model, polarization variation across pulse profile) is different from what is obtained for white dwarfs.